DAMAGE MODEL FOR THE COMPOSITE MATERIAL UNDER MULTIAXIAL LOADING

P.A. Dodonov[1], N.N. Fedonyuk[1]

[1]The Krylov State Research Centre, St. Petersburg, Russia
Email: krylov@krylov.spb.ru, Web Page: http://www.krylov-center.ru/

Keywords: damage model, multi-axial loading, experiment, non crimp fabrics

Abstract
In this investigation we examine the properties of the layered composite materials made of biaxial non crimp fabrics. To analyze it we propose modifications to Ladevèze material model of the unidirectional ply and determine the model's parameters under multi-axial loading. The complex material model initially incorporates plasticity, failure and damage mechanisms. The modified model separates the damage evolution law from the failure criterion, leaving only an indirect link through stress values. Failure mechanism of the initial damage material was reviewed and replaced by unsophisticated stress-based failure criterion. Multi-axial loading was conducted using the test procedure created based on "Arcan" method. Nonlinear behavior under multi-axial loading was analyzed using numerical models and compared with the experimental results.

1. Introduction

Hull marine structures operate in severe environments and are designed to endure under complex loading. The supporting elements are usually designed relatively thick, multilayered with intricate scheme of reinforcement to withstand hard operational load. Production of these structures is always consistent with development of materials due to the logic of the unified technological process. The studying of damaging processes and fracture mechanisms of composite materials under various types of loading allows us to increase efficiency of material use and introduce scientifically based strength standards. Prediction of mechanical behavior of the constructions using the latest numerical methods is part of this study.

Considered composite materials are produced from multiaxial fabrics made of unidirectional fiber layers laid-at various angles and impregnated with epoxy vinyl ester resin using RTM and VARTM methods. This method allows us to create large hull marine structures with combinations of layered fiber reinforced plastic (FRP). It features high technological effectiveness and relatively low labor consumption.

The goal of this analysis was to create the mathematical model that could predict mechanical properties of FRP combined of random number of random non crimp fabrics (NCF) with known mechanical properties. To provide proper precision of the model it had to consider the mechanical processes that are describing the behavior of composite material's microstructure. Damage model was chosen due to its ability to include in consideration different aspects of nonlinear behavior and the option to use it in finite-element models to calculate the full-scale elements of hull structure. The conducted analysis of experimental data showed the necessity of modifications to the original model.

The challenge was to compute the damaged state of a composite structure subjected to complex multiaxial loading until final fracture. Damage refers to the development of micro voids and micro

Excerpt from ISBN 978-3-00-053387-7

cracks, which lead to macro cracks and then to rupture. For such materials, damage is generally of a highly complex nature. There's not one single, but rather several, damage mechanisms which are highly anisotropic due to the microstructure and meso structure of the composite material (see Fig. 1). Brittle fracture and progressive damage growth with plastic strain are both present.

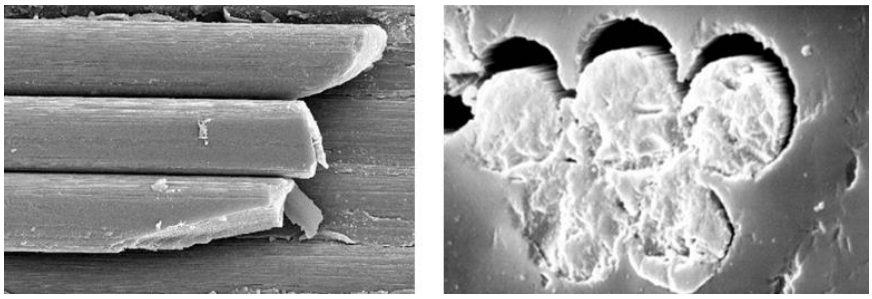

Figure 1. Composite microstructure leads to diverse damage mechanisms [11].

2. Damage model

Main set of concepts and tools of the damage mechanics was introduced by L.M.Kachanov [1] and Y.N.Rabotnov [2]. The presented analysis is based on P.Ladevèze damage model [3] which uses damage indicators as internal damage variables:

$$\begin{cases} d_i = 1 - \dfrac{E_i}{E_i^0} \\ d_{12} = 1 - \dfrac{G_{12}}{G_{12}^0} \end{cases} \tag{1}$$

The damaged material strain energy $\boldsymbol{E}_D$ of the unidirectional ply (see Fig. 2) is written in the modified form to include the compressive stresses into the damaging process:

$$\boldsymbol{E}_D = \frac{1}{2}\left[\frac{{\sigma_1}^2}{E_1^0\left(1-d_1\right)} + \frac{{\sigma_2}^2}{E_2^0\left(1-d_2\right)} + \frac{{\tau_{12}}^2}{G_{12}^0\left(1-d_{12}\right)} \right] \tag{2}$$

Here E^0_i and G^0_{12} are the elastic moduli in the initial state, σ_1, σ_2 and τ_{12} are the components of stress tensor in plane of the ply in coordinate system (CS) correlating with fiber orientation.

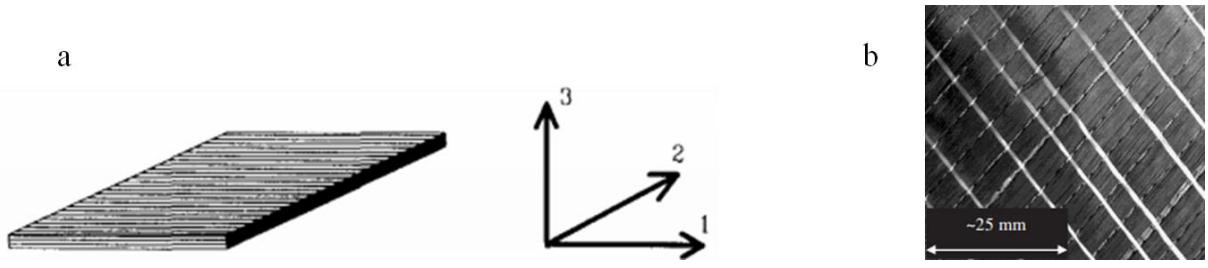

Figure 2. a) Unidirectional fiber reinforced ply with associated coordinate system;
b) 2-layer biaxial $[\pm 45^o]_{2s}$ non-crimped fabric [11].

Excerpt from ISBN 978-3-00-053387-7

The damage evolution law is defined based on experiments and in our case written as follows:

$$\begin{cases} d_{12} = d_{12}^{sat.} - Be^{-\omega\sqrt{Y}}, & Y \geq Y_0 \\ d_{12} = 0, & Y < Y_0 \\ d_2 = b_3 d_{12}, & Y_{d2} < Y_{d2c} \\ d_1 = 0, & Y_{d1} < Y_{d1c(+/-)} \end{cases} \quad (3)$$

Here Y is the equivalent thermodynamic force; Y_0 is the threshold of the damaging process; $Y_{d1c(+/-)}$ and Y_{d2c} are the critical thermodynamic forces for the loading; Y_{di} and Y_{d12} are associated with the internal damage variables:

$$\begin{cases} Y = b_2 Y_{d2} + Y_{d12} \\ Y_{di} = \dfrac{\partial \boldsymbol{E}_D}{\partial d_i} = \dfrac{\sigma_i^{\,2}}{2E_i^0\left(1-d_i\right)^2} \\ Y_{d12} = \dfrac{\sigma_{12}^{\,2}}{2G_{12}^0\left(1-d_{12}\right)^2} \end{cases} \quad (4)$$

The damage evolution law (3) requires material constants $d_{12}^{sat.}$, B and ω which are defined based on tension tests with ±45° cross-ply laminates [3]. In the current analysis these tests were replaced with the shear test with v-notched rail shear tests [4]. Coupling constants b_2 and b_3 are harder to determine. They are usually calculated based on an additional set of experiments with ±67.5° cross-ply laminates that are produced with exact same material of unidirectional layers [3]. In case of NCF the manufacturing of such test specimen could be close to impossible, since the modification to fabric's structure leads to a different characteristics of biaxial fabrics, impregnation and ultimately to deviation of mechanical properties. Alternatively b_2 and b_3 could be evaluated based on analytical models of unidirectional FRC layer which consider micromechanical processes on matrix/fiber interfaces [3] but the precision of this analytical method could be questioned. In the current study the coupling constants were defined using the cyclic multiaxial test and details are presented below. The first formula in (3) is the result of best approximation of our experiments, conducted with non-crimp fabrics. The damage evolution law takes different forms in different studies [3, 5, 6]. The saturation parameter $d_{12}^{sat.}$ allows model to achieve high shear stresses after initiation of damaging process. Critical thermodynamic forces $Y_{d1c(+/-)}$ and Y_{d2c} are calculated separately based on ultimate strengths of material. Failure criterion is discussed below.

Material shows the growth of residual strain that could be explained by plastic-like behavior of the material under shear and transverse loading. The coupling between the damage and plasticity is taken into account by consideration of the effective stresses $\tilde{\sigma}_2$, $\tilde{\tau}_{12}$ and effective strains $\tilde{\gamma}_{12}$, $\tilde{\varepsilon}_2$ in plastic flow equation. The effective stress and the rate of effective strain are defined as:

$$\begin{aligned} \tilde{\tau}_{12} &= \tau_{12}/\left(1-d_{12}\right) & \tilde{\sigma}_2 &= \sigma_2/\left(1-d_2\right) \\ \dot{\tilde{\gamma}}_{12} &= \dot{\gamma}_{12}\left(1-d_{12}\right) & \dot{\tilde{\varepsilon}}_2 &= \dot{\varepsilon}_2\left(1-d_2\right) \end{aligned} \quad (5)$$

The elastic domain is described by Von Mises yield criteria with an associated flow rule that is used to describe the evolution of residual plastic strains in the matrix caused by the transverse and shear strain components:

$$f\left(\tilde{\sigma},\, \tilde{p}\right) = \sqrt{\tilde{\sigma}_{12}^{\,2} + \left(a\tilde{\sigma}_2\right)^2} - \left(K\tilde{p}^{\,y} + R_0\right) \quad (6)$$

Here K, R_0 and y represent the shape of the equivalent plastic strain curve. Factor a^2 can account for material anisotropy. Assuming an isotropic matrix material it can be shown from the Von Mises yield condition that $a^2 = 1/3$ [5].

The failure model of the Ladevèze damage model is described by set of critical thermodynamic forces $Y_{d1c(+)}$, $Y_{d2c(+)}$, $Y_{d1c(-)}$ and Y_{d12c} that serve as the set of ultimate tensile and compressive strengths

Excerpt from ISBN 978-3-00-053387-7

values[3, 6]. It requires an additional compressive strength condition to create limitation for $\sigma_2 < 0$ and generally works as the unneeded sophistication. The latter conclusion was reached when the comparison to the traditional stress-based failure criteria of was conducted. The adaptation of maximum stress criterion made by P. Zinoviev [7, 8] showed identical results to failure criteria of the damage model. Our modification of the maximum stress failure criterion is written as:

$$\begin{aligned} &d_1 = 1 \;\&\; d_{12} = 1 \;\&\; d_2 = 1, \qquad if \;\; \sigma_1 = \sigma_{1\_UTS(UCS)} \\ &d_1 = 0 \;\&\; d_{12} = 1 \;\&\; d_2 = 1, \qquad if \;\; \sigma_2 = \sigma_{2\_UTS(UCS)} \\ &d_1 = 0 \;\&\; d_{12} = 1 \;\&\; d_2 = 1, \qquad if \;\; \tau_{12} = \tau_{12c\_USS} \end{aligned} \tag{7}$$

Here σ_{1UTS}, σ_{1UCS}, σ_{2UCS}, σ_{2UCS} and τ_{12USS} are the ultimate strengths of the ply material. The failure model in form (7) doesn't require any additional calculations of critical thermodynamic forces. It introduces ultimate compressive strength for transverse stress component σ_2.

3. Multi-axial loading experiment

3.1. Fixture for the multi-axial loading experiment

To conduct the experiments we designed and produced special fixture (see Figure 3a and 3c) based on combination of the v-notched rail shear test [4] and the idea of Arcan test method [9]. The Arcan method doesn't have any standard design for the test and to create this fixture the ASTM D 7078's design was taken as base design: both the dimensions of specimen and method to constrain it in the fixture are similar to the standard [4]. The produced test method creates fixed relation between the longitudinal and shear forces that act in the middle section of the specimen. Mean values of the stress components were considered. The longitudinal stress σ_x and shear stress τ_{XY} in CS of the specimen are calculated using angle β (see Figure 3a):

$$\sigma = \frac{P}{bh}, \qquad \begin{cases} \tau_{xy} = \sigma \cos(\beta) \\ \sigma_x = \sigma \sin(\beta) \\ \sigma_y = \lambda \sigma \sin(\beta) \end{cases} \tag{8}$$

Here b and h correspond to width and height of specimen's middle section, P represents the loading force. Angle β measures the deviation of specimen's orientation from the direction of load. Separate finite element analysis showed the necessity to consider the transverse σ_y stress which cannot be defined only by external load and fixture's angle β. The approximation presented in (8) introduces the coefficient λ which includes the impact of material's elastic properties, and specimen's shape. In case of anisotropic material coefficient λ also depends on fixture's angle β.

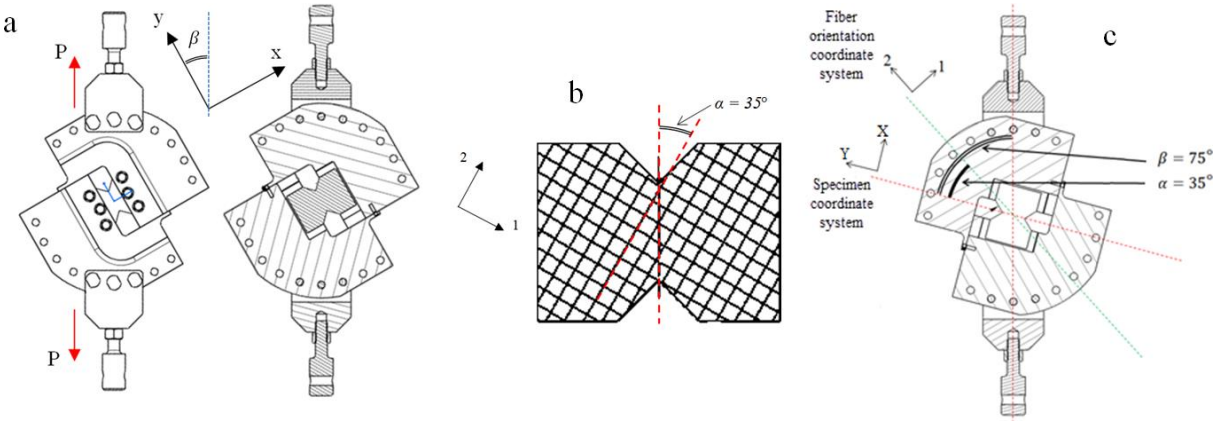

Figure 3. Design of test fixture for multiaxial loading: a) specimen in relation to loading direction; b) rotation scheme for fiber orientation out of specimens made of biaxial NCF; c) angles α and β.

Excerpt from ISBN 978-3-00-053387-7

3.2. Fiber orientation of the specimen

Rotation scheme is presented on Figure 3b. Considered materials are made of biaxial NCF with orthogonal fiber orientations and the hatching lines correspond to these orientations. The rotation of the fiber orientation for the specimen provides with the opportunity to select required relations between the stress components $\bar{\sigma}_1$, $\bar{\sigma}_2$ and $\bar{\tau}_{12}$. The overline mark denotes the attachment to the stresses and strains of the of biaxial FRP material. Transformation of equations (8) is required to calculate the stress components considering the rotation angle α. Various combinations of angles α and β were proposed. For example, one of them is presented on the Figure 4a.

4. Results

4.1. Results of experiments

The experiments were prepared and performed to achieve the values for constants of the damage model. The damage evolution law (3) was approximated using the results of the cyclic test α=0◦ and β=0◦ shear loading test. To calculate the coupling coefficients following test was conducted and analyzed. Optical measurement system Gom Aramis was used to get the deformation field of the specimen. An example of the acquired results is presented on the Figure 4a. The shear strain field was calculated and presented on top of the deformed specimen of carbon fiber reinforced plastic (CFRP). Figure 4b shows shear strain field in CS of the specimen for the combination of tension and shear loadings which corresponds: angles α=35◦ and β=75◦ of glass fiber reinforced plastic (GFRP). In both types of tests values of strain components were measured in the middle of the narrowed section and averaged on the area 2x2 mm. Both types of tests showed uniform strain fields in the narrowed section of the specimen.

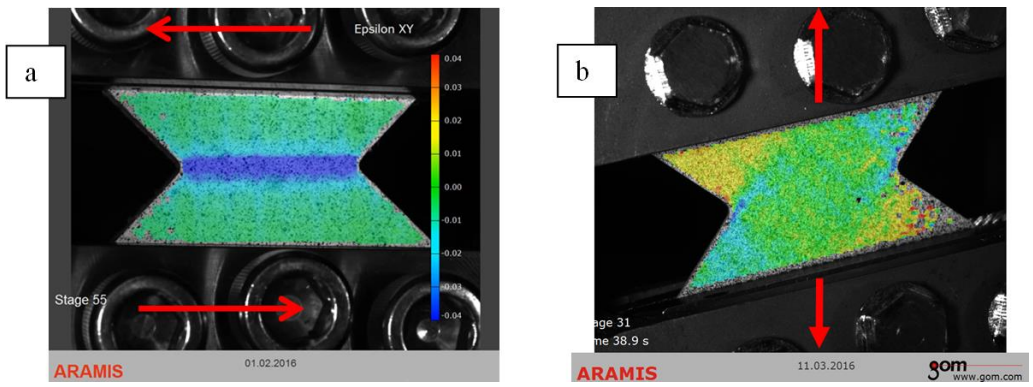

Figure 4. Contour plot of shear strain ε_{xy} field plotted on top of specimens a) during pure shear loading test of the CFRP α=0◦ and β=0◦; b) during combined tension and shear loading of GFRP α=35◦ and β=75◦. Red arrows show the direction of displacement of the metal parts applying the load.

Strain measurements were compared with calculated values of stresses $\bar{\sigma}_1$, $\bar{\sigma}_2$ and $\bar{\tau}_{12}$ and as the result the diagrams of the Figure 5 were plotted. In case of GFRP presented on Figure 4b the coefficient λ from eq. (8) was taken equal to 0.44. The shear strain $\bar{\gamma}_{12}$ shows highly nonlinear behavior with plastic residual strain and the lowering of elastic moduli, while the normal components of strain $\bar{\varepsilon}_1$ and $\bar{\varepsilon}_2$ provide with much smaller strain values and their behavior is relatively linear. The small nonlinearity in fiber directions could be explained by the deviations in actual angles α и β, and the effect of turned fibers during accumulation of large strains in shear.

Excerpt from ISBN 978-3-00-053387-7

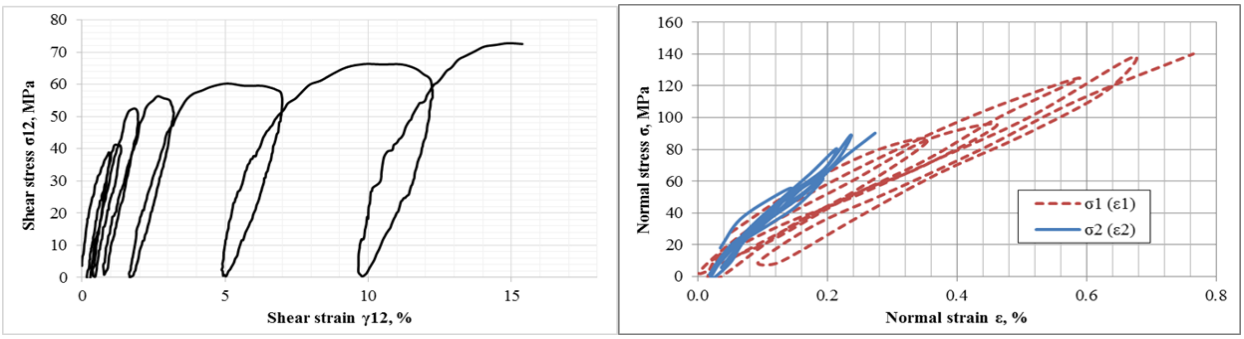

Figure 5. Stress - Strain diagrams of the biaxial GFRP cyclic test under multi-axial loading (combination of angles α=35◦ and β=75◦).

To calculate coupling coefficients the damaging indicator $\bar{d}_{12}$ was calculated at each cycle of the multiaxial load. Like in previous case, the overline mark denotes the attachment to the biaxial FRP material. In following equations the properties of the biaxial FRP were used to simplify the mathematical calculations. The assumption that biaxial FRP has the same shear properties as the unidirectional plies from which it is made of was used $\bar{d}_{12}$ = d_{12}. Also thermodynamic forces $\bar{Y}_{di}$, $\bar{Y}_{d12}$ for the biaxial FRP are calculated on each loading cycle:

$$\begin{cases} \bar{Y}_{di} = \dfrac{\bar{\sigma}_i^{\,2}}{2\bar{E}_i^0\left(1-\bar{d}_i\right)^2} \\ \bar{Y}_{d12} = \dfrac{\bar{\tau}_{12}^{\,2}}{2\bar{G}_{12}^0\left(1-\bar{d}_{12}\right)^2} \end{cases} \tag{9}$$

Here $\bar{E}_i^0$ and $\bar{G}_{12}^0$ are the elastic moduli of the biaxial FRP. Calculated values (9) are required to determine the coupling coefficient A of a damage model for fabrics. It was introduced by C. Hochard [10] with the following relation between the coupling coefficients A and the b_2:

$$b_2 = \frac{2E_1^0 A}{E_2^0\left(1+\nu_{12}\right)^2} \tag{10}$$

$$A = \frac{ln^2\left(\dfrac{d_{12}^{sat.}-d_{12}}{B}\right)-\omega^2\bar{Y}_{d12}}{\omega^2\left(\bar{Y}_{d1}+\bar{Y}_{d2}\right)} \tag{11}$$

So coupling coefficient A could defined by the values of d_{12}, $\bar{Y}_{d1}$ and $\bar{Y}_{d2}$ on every cycle of multiaxial loading. Constants $d_{12}^{sat.}$, B and ω of the damage evolution law (3) were defined earlier from "pure shear" loading tests. Logarithmic solution in (11) is present as the consequence of approximation choice (3). The combination of (10) and (11) provides the following equation for b_2:

$$b_2 = \frac{2E_1^0\left(ln^2\left(\dfrac{d_{12}^{sat.}-d_{12}}{B}\right)-\omega^2\bar{Y}_{d12}\right)}{E_2^0\left(1+\nu_{12}\right)^2\omega^2\left(\bar{Y}_{d1}+\bar{Y}_{d2}\right)} \tag{12}$$

4.2. Numerical results

The modified damage model was introduced in the numerical code to simulate the loading of multilayered FRP laminates. As an example of properties for the FRP used in the analyses the damage evolution law is shown on figure 6a with resulting stress strain curve on figure 6b.

Excerpt from ISBN 978-3-00-053387-7

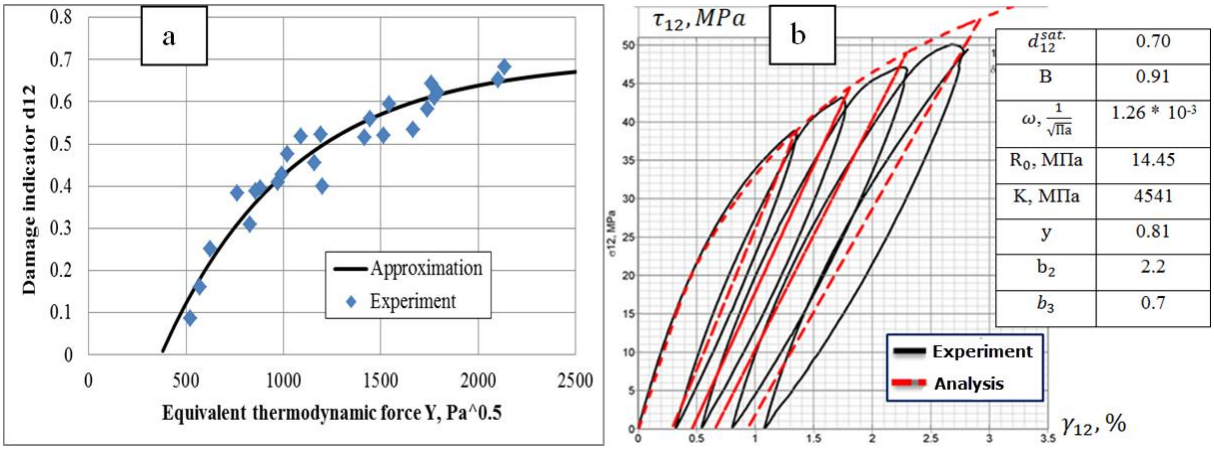

Figure 6. Experiment in comparison to the a) approximation of damage evolution law; b) shear stress-strain diagram for the GFRP.

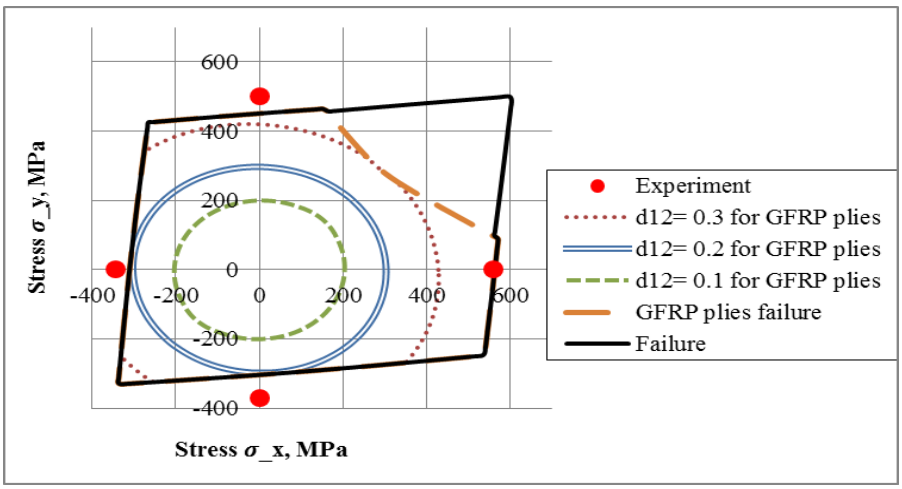

Figure 7. Failure criteria surface for hybrid glass+carbon FRP (carbon fabric + glass fabric $[[0^\circ/90^\circ]_{2s}\ [+/-45^\circ]_{2s}]_s$); damage evolution surfaces for glass fiber layers are presented.

4.3. Mechanical properties of the multilayered hybrid FRP

Two FRP materials were made of a mixes of a layers of different fabrics (creating two hybrid FRPs). Fabrics were combined to acquire quasi isotropic FRP. Mechanical properties were tested in the series of experiments and compared with the results of the numerical analysis. The results are presented in table 1. Ultimate Tensile Stresses (UTS) are predicted with deviation of a less than 10% for both hybrid materials. Numerical results for the Ultimate Compressive Stresses (UCS) are less accurate and provide with higher deviation. The compressive stress tests were conducted by different standards and different specimen types were used. Same material showed discrepancy in experimental results that was comparable with the deviation from numerical results. Numerical results are also presented on the figure 7. Failure criteria for the FRP made of combination of glass fiber NCF layers and carbon fiber NCF layers is shown in comparison with the experimental results. Layers of glass fiber NCF are subjected to damaging process. To represent the damage evolution in these layers the surfaces of equal damage indicator value d_{12} are presented. Shape of damage evolution surfaces could remind of the quadratic failure criteria shapes while the actual shape of the ultimate failure is almost perfectly piecewise linear. This effect shows that the damaging process is hidden in the elastic-like deformation of quasi-isotropic multiaxial FRP.

Excerpt from ISBN 978-3-00-053387-7

Table 1. Results of experiments in comparison with the analytical results for two types of hybrid FRP.

Specimen Type	*Glass + Carbon FRP* $[[0^\circ/90^\circ]_{2s}\ [+/-45^\circ]_{2s}]_s$			*Carbon + Carbon FRP* $[[0^\circ/90^\circ]_{2s}\ [+/-45^\circ]_{2s}]_s$		
	Test (MPa)	Analysis (MPa)	Deviation (%)	Test (MPa)	Analysis (MPa)	Deviation (%)
UTS 0^o	560	562	0.4%	563	605	7.5%
UTS 90^o	500	451	-9.8%	531	487	-8.3%
UCS 0^o	343	310	-9.6%	364	335	-8.0%
UCS 90^o	370	303	-18.1%	–	328	–

5. Conclusions

The damage models of the fiber reinforced plastics were analyzed and modified to describe the mechanical properties of the plastics made of non-crimp fabrics. Using the analytical model we assumed that the balanced FRP is composed of two plies with similar properties. Maximum stress failure criterion was combined with the damage evolution model. Special fixture was developed to perform the combined "shear-tension" loading. Results of multi axial cyclic loading experiments were analyzed to extract the material constants for the model. Developed method was used to predict the effective ultimate strengths of hybrid FRP made of combination of various fabrics. Calculated data was compared with test results.

References

[1] L. M. Kachanov. Time of the rupture process creep conditions, *Izv Akad Nauk S.S.R. Otd, Tech. Nauk*, 8: 26-31, 1958.
[2] Y. N. Rabotnov. Creep rupture. *Proc. XII. Int. Cong. Appl. Mech*. Stanford-Springer, 1968.
[3] P. A. Ladevèze. Damage computational method for composite structures. *Computer Structures*, vol. 44, 1992.
[4] D.O. Adams, J.M. Moriarty, A.M. Gallefos and D.F. Adams. Development and Evaluation of the v-notched rail shear test for composite laminates, *Federal Aviation Administration Report DOT/FAA/AR-03/63, FAA Office of aviation Research, Washington, D.C.,* 2003.
[5] L. Greve, A.K. Pickett. Modelling damage and failure in carbon/epoxy non-crimp fabric composites including effects of fabric pre-shear. *Composites: Part A,* 37: 1983–2001, 2006.
[6] P. Ladeveze, E. Le Dantec. Damage modelling of the elementary ply for laminated composites. *Composites Science and Technology,* 43: 257-267, 1992.
[7] P. Zinoviev, S.V. Grigoriev, O.V. Labedeva, L.R. Tairova. Strength of multilayered composites under plane stress state. *Composite Science Technology,* 58:1209–24, 1998.
[8] P. D. Soden, A. S. Kaddour and M. J. Hinton, Recommendations for designers and researchers resulting from the world-wide failure exercise, *Failure Criteria in Fibre Reinforced Polymer Composites*, 1223- 1251, 2004.
[9] M. Arcan, Z. Hashin, A. Voloshin, A Method to Produce Uniform Plane-stress States with Applications to Fiber-reinforced Materials. *Experimental mechanics*, 18(2): 141-146, 1978.
[10] C. Hochard, P-A. Aubourg and J-P Charles. Modelling of the mechanical behaviour of woven-fabric CFRP laminates up to failure, *Composites Science and Technology*, 61: 221-230, 2000.
[11] P. Lundmark and J. Varna. Constitutive relationships for damaged laminate in in-plane loading. *Int. J. Dam. Mech.*, 14(3): 235-259, 2005.

Excerpt from ISBN 978-3-00-053387-7